Preprints.org

Article

Not peer-reviewed version

Co-Hydrothermal Carbonization of Cacao (*Theobroma cacao*) Shells with LDPE: Hydrochar Characterization, Comparative Pyrolytic Kinetic Study, and Thermodynamic Property Determination

Mariane Fe A. Abesamis , Alec Paolo V. Dy Pico , Rosanne May E. Marilag , Javinel P. Servano , Queenee Mosera M. Ibrahim , Cymae O. Oguis , Alexander Q. Bello Jr. , Kenth Michael U. Uy , Joevin Mar B. Tumongha , Rodel D. Guerrero , Ralf Ruffel M. Abarca , Alexander O. Mosqueda *

Posted Date: 3 March 2026

doi: 10.20944/preprints202603.0200.v1

Keywords: LDPE; cacao shell (CS); hydrochar; hydrothermal carbonization (HTC); co-hydrothermal carbonization (co-HTC)

Preprints.org is a free multidisciplinary platform providing preprint service that is dedicated to making early versions of research outputs permanently available and citable. Preprints posted at Preprints.org appear in Web of Science, Crossref, Google Scholar, Scilit, Europe PMC.

Copyright: This open access article is published under a Creative Commons CC BY 4.0 license, which permit the free download, distribution, and reuse, provided that the author and preprint are cited in any reuse.

Preprints.org (www.preprints.org) | NOT PEER-REVIEWED | Posted: 3 March 2026 doi:10.20944/preprints202603.0200.v1

Disclaimer/Publisher's Note: The statements, opinions, and data contained in all publications are solely those of the individual author(s) and contributor(s) and not of MDPI and/or the editor(s). MDPI and/or the editor(s) disclaim responsibility for any injury to people or property resulting from any ideas, methods, instructions, or products referred to in the content.

Article

Co-Hydrothermal Carbonization of Cacao (*Theobroma cacao*) Shells with LDPE: Hydrochar Characterization, Comparative Pyrolytic Kinetic Study, and Thermodynamic Property Determination

Mariane Fe A. Abesamis [1], Alec Paolo V. Dy Pico [1], Rosanne May E. Marilag [2], Javinel P. Servano [2], Queenee Mosera M. Ibrahim [2], Cymae O. Oguis [2], Alexander Q. Bello, Jr. [2], Kenth Michael U. Uy [1], Joevin Mar B. Tumongha [1], Rodel D. Guerrero [1,2], Ralf Ruffel M. Abarca [1,2] and Alexander O. Mosqueda [1,2,*]

[1] Waste Valorization and Energy Laboratory, Center for Energy Research and Technology, Mindanao State University – Iligan Institute of Technology, Andres Bonifacio Avenue, Iligan City, 9200 Philippines

[2] Department of Chemical Engineering and Technology, College of Engineering, Mindanao State University-Iligan Institute of Technology, Iligan City 9200, Philippines

* Correspondence: alexander.mosqueda@g.msuiit.edu.ph

Abstract

In the Philippine agricultural setup, pre-harvest cacao (*Theobroma cacao*) fruits are wrapped with low-density polyethylene (LDPE) for moisture retention and damage protection. Responding to the growing concern for its waste volume and scarcity of treatment, this research explores the co-hydrothermal carbonization (co-HTC) of cacao shells (CS) and LDPE as a method to convert agricultural waste with plastic into hydrochar of potential energy applications. Thus, observations on the thermal, physicochemical, and morphological changes from feedstocks to hydrochar are carried out. Optimal conditions of 200 °C for 60 minutes resulted in hydrochar with 21.11 MJ/kg and appreciable thermal properties. SEM micrographs show rough and porous structures of hydrochar powder and presence of cracks on oversized LDPE film, while EDX analysis reveals C, K, Ca, and Zn metals that affects chemical pathway. FTIR analysis further supports chemical synergy by preservation of functional groups innate from both parent materials, as well as relative LDPE degradation due to chain scissoring and oxidative reactions. Kinetic and thermal evolutions are also investigated to reveal influence of pretreatment to the stability of cacao shells-dominated hydrochar and the effectivity of biomass integration to facilitate relatively easier degradation of LDPE. The findings support co-HTC as a viable technology to enhance the circular economy by valorizing LDPE and cacao shells while promoting energy recovery.

Keywords: LDPE; cacao shell (CS); hydrochar; hydrothermal carbonization (HTC); co-hydrothermal carbonization (co-HTC)

1. Introduction

Plastics have been produced and used for a variety of applications in different industries throughout the world. From a plastic production of about 2 million tons in 1950, it climbed up to a worldwide scale of 400.3 million tons in 2022 and is thus expected to exponentially increase in the coming years [1]. However, they also constitute a major threat to the environment due to their resistance to degradation. The degradation of plastics takes much time, ranging from several decades to hundreds of years [2].

The worldwide annual production of non-degradable plastic ranges from 350 million to 400 million tons. In 2020 alone, nearly 400 million tons of plastics were produced globally [3]. Of this, 5

© 2026 by the author(s). Distributed under a Creative Commons CC BY license.

Preprints.org (www.preprints.org) | NOT PEER-REVIEWED | Posted: 3 March 2026 doi:10.20944/preprints202603.0200.v1

to 13 million tons of waste plastic yearly are released into the ocean, which has negative consequences to ecology [4,5].

Globally, only 18% of plastics waste are recycled, and 24% are incinerated. The remaining 58% are either landfilled or enter the natural environment, where plastics accumulate and persist for a long period of time [3]. These wastes release toxins into the soil, water, and air as they weather and react with the natural environment through different mechanisms such as with UV radiation, heat, pressure, interaction with chemicals, as well as with living organisms [3,5].

Polyethylene and polypropylene represent about 92% of the synthetic plastics produced, and they are used for production of plastic bags, disposable containers, bottles, packaging materials, etc. One particular application of polyethylene, particularly low-density polyethylene (LDPE), is the protective sleeve for cacao fruits. The primary impediment encountered in cacao production is the impact of insects that feed on cacao leaves and fruits. To effectively safeguard the cacao fruit, a recommended approach is to use LDPE sleeves.

Cacao production generates substantial waste, with approximately 80% of the cacao fruit discarded, including shells and pod husks, which are often [6]. Cacao shells (CS) with attached LDPE sleeves are usually disposed of in low-lying areas or landfills, with a fraction subjected to incineration. In response to this underlying concern, a promising approach has emerged, involving the conversion of such waste materials into hydrochar, a coal-like product, through the application of a hydrothermal carbonization (HTC) process [7].

Interestingly, studies have shown that biomass and plastics make up an effective solid fuel when converted into hydrochar [8]. For instance, Islam et al. (2021) investigated the co-HTC of corn stover with waste polyurethane at varying ratios and temperatures. The co-HTC process effectively reduced the nitrogen and oxygen content, improving the overall fuel quality of hydrochar [9]. Another study by Wang et al. (2023) examined the co-HTC of polyvinyl chloride (PVC) with various lignocellulosic biomasses, including pine, bamboo, corncob, wheat stalk, and corn stalk. The study revealed that the interactions between PVC and biomass components enhanced the fuel properties and combustion behaviors of the resulting hydrochars [10]. Moreover, co-HTC has been shown to effectively reduce ash content and enhance the grindability and combustion properties of hydrochar, making it a viable alternative to fossil fuels in various applications [11]. Additionally, HTC has been effective in reducing the inorganic content of biomass, which would have led to operational issues such as slagging and fouling during combustion or pyrolysis. By decreasing the ash content, HTC pretreatment mitigates these problems, as evidenced by the findings of Wang et al. (2023) [10].

However, co-processing plastics also introduces complexities, including phase separation, formation of tar or waxy residues, and operational challenges like reactor clogging or inconsistent product quality. These factors highlight the need for optimized feedstock blending ratios, pre-treatment, and controlled operating conditions to fully harness the benefits of plastics in WTE applications

Furthermore, the co-HTC of CS and their attached LDPE sleeves have not been investigated, and its effect on the degradation of LDPE has not yet been explored. Therefore, this study aims to investigate the degradation of LDPE with CS via co-HTC.

2. Materials and Methods

2.1. Sample Preparation

Cacao shells and LDPE were obtained from post-harvest processing residues of cacao (*Theobroma cacao*) from a farm in Davao City. The LDPE sleeves collected from each cacao fruit were carefully removed and preserved for subsequent analysis. To facilitate the separation of the cacao shells from the pulp and seeds, the fruits were subjected to sun-drying. After sufficient drying, the fruits were cut open and manually deseeded, with the seeds discarded. The empty cacao shells were then weighed and cut into small 1-2 cm cubes. The drying process was conducted at a 105 °C for a week. The raw cacao shells were weighed, and their total mass was documented both before and after

© 2026 by the author(s). Distributed under a Creative Commons CC BY license.

Preprints.org (www.preprints.org) | NOT PEER-REVIEWED | Posted: 3 March 2026 doi:10.20944/preprints202603.0200.v1

drying to monitor moisture loss. Once fully dried, the dried cacao shells were stored in breathable cloth bags to prevent reabsorption of moisture during storage. The collected LDPE sleeves were also cut into 1 cm by 1 cm strips in preparation for subsequent experimental procedures.

2.2. Co-Hydrothermal Carbonization

Co-HTC experiments involving CS-LDPE samples were conducted using an autoclave reactor. Weight composition of CS and LDPE was set as retrieved from LDPE sleeve of raw cacao fruit and the deseeded cacao shell which is 98% CS and 2% LDPE. The raw feedstocks were prepared in a mass ratio with water of 1:8, respectively. A measured 80 mL of distilled water was added to the mixture, which was then transferred into a large boiling tube and placed into the autoclave reactor positioned within a fume hood. The autoclave was then purged with 99.99% high purity nitrogen gas to simulate an oxygen-free environment. After the autoclave was sealed, it was heated up to the predetermined reaction temperature and kept there for 60 minutes. After the reaction, the autoclave was quenched to room temperature with running water. The resulting product was then removed from the autoclave and vacuum-filtered. The resulting solid hydrochar product was washed with distilled water and oven-dried for 24 hours at 105 °C before they were stored hermetically. After drying, the mass of the resulting hydrochar yield was determined and its % mass yield was calculated using Equation (1) shown below.

$$MY, \% = \frac{m_{HC}}{m_{raw\ feed}} \times 100 \quad (1)$$

2.3. Experimental Design and Statistical Analysis

For the co-HTC optimization experiments, Response Surface Methodology with Central Composite Design (CCD) was employed to observe the relationships between the co-HTC parameters (reaction temperature and residence time) and the resulting % hydrochar mass yield. Shown in Table 1 were the factor levels and desired response for the co-HTC of CS with LDPE using the CCD. The significance of each of these parameters to the response was determined using two-way analyses of variance (ANOVA).

Table 1. Summary of Experimental Design.

Reaction Parameter	-1 Level	+1 Level	Response
Reaction Temperature	200 °C	240 °C	Mass Yield (%)
Residence Time	30 minutes	60 minutes	

2.4. Optimization of Co-HTC Experiment Parameters

Optimization of the reaction parameters was done aiming to maximize the % hydrochar mass yield, determining the optimum reaction temperature and residence time. After determining these parameters, two more HTC runs were performed following these parameters and were then subjected to characterization and further analyses.

2.5. Characterization of Optimized Hydrochar

Hydrochar fractions derived from co-HTC were separated based on particle size distribution. The three (3) samples labeled as: (1) Undersized Hydrochar (less than 100 microns), (2) Oversized Hydrochar (greater than 100 microns), (3) Oversized LDPE. The resulting samples from co-HTC pretreatment were deployed for characteristic examination through analytical techniques: Bomb Calorimetry for HHV, Fourier Transform Infrared Spectroscopy (FTIR) for identification of functional groups and assessment of changes in chemical composition, and Scanning Electron Microscopy-Energy Dispersive X-ray (SEM-EDX) for analysis of the surface morphology and determination of the elemental composition.

© 2026 by the author(s). Distributed under a Creative Commons CC BY license.

Preprints.org (www.preprints.org) | NOT PEER-REVIEWED | Posted: 3 March 2026 doi:10.20944/preprints202603.0200.v1

2.6. Thermal Analysis via Pyrolysis of Hydrochar Fractions

To assess the thermal behavior and pyrolytic potential of each hydrochar fraction, the samples underwent Thermogravimetric Analysis (TGA) using a TGA 4000 instrument (PerkinElmer Inc.). TGA was conducted with samples being heated from 40 °C to 660 °C under continuous flow of nitrogen gas at 20 mL/min. to maintain an inert environment. The heating rate was set to 20 °C/min. The TGA instrument continuously recorded mass loss, generating thermogravimetric and decomposition stages, and evaluating thermal stability. This data is critical in understanding the pyrolysis performance and energy recovery capability of the hydrochar.

Thermogravimetric Analysis (TGA) via pyrolysis utilizes pyrolysis kinetics modeling in examining the pyrolysis mechanism of a feedstock such as biomass. In thermal analysis, a widely used non-isothermal model-fitting technique that assumes the degree of the reaction order, which the Taylor series expansion is used for the arrangement of the integral, is known as the Coats and Redfern (CR) equation. It assumes a simplified single-step reaction mechanism, averaging out complexities The linear representation of this method is presented in Equation (2):

$$\ln\left[\frac{g(\alpha)}{T^2}\right] = \ln\left[\frac{AR}{\beta Ea}\left(1-\frac{2RT}{Ea}\right)\right] - \frac{Ea}{RT} \quad (2)$$

where, g(α) is the integral form of the kinetic model, T is the absolute temperature (K), A is the pre-exponential factor (min^{-1}), β is the heating rate (K/min), Ea is the activation energy (J/mol or kJ/mol), and R is the universal gas constant (8.314 J/mol·K).

From the linear plot of the left side of Equation (2) and 1/T, the slope and intercept can be used to identify the kinetic parameters. The activation energy Ea is determined from the line's slope (Yan et al., 2014), while the pre-exponential factor A comes from its intercept. The temperature-dependent rate constant k therefore can be achieved using Arrhenius equation:

$$k = Aexp^{\left(\frac{-Ea}{RT}\right)} \quad (3)$$

Several kinetic models listed in Table 2 were evaluated, and the model with the highest coefficient of determination was selected as the best fit.

Table 2. Mathematical expressions for g(α) according to different solid state reaction mechanism models.

Mechanism		g(α)	Code
Power Law	n= ½	$\alpha^{1/2}$	P2
	n= 1/3	$\alpha^{1/3}$	P3
	n= ¼	$\alpha^{1/4}$	P4
Chemical Reactions	First order	-ln(1-α)	R1
	One-a-half order	2[(1-α)$^{-1.5}$–1]	R1.5
	Second order	[1/(1-α)]-1	R2
Diffusion Reaction	One-dimensional diffusion	α^2	D1
	Two-dimensional diffusion	(1-α)-ln(1-α)+α	D2
	Three-dimensional diffusion - Jander	[1-(1-α)$^{1/3}$]^2	D3
	Three-dimensional diffusion – Gistling-Brounsthein	$(1-\frac{2\alpha}{3})$-(1-α)$^{2/3}$	D4
Phase Interfacial Reaction	One dimension	α	P1
	Two dimensions (Cylindrical)	1-(1-α)$^{1/2}$	C1
	Three dimensions (Sphere)	1-(1-α)$^{1/3}$	C2
Nucleation and Growth Reaction	Two-dimensional	[-ln(1-α)]$^{1/2}$	A2
	Three-dimensional	[-ln(1-α)]$^{1/3}$	A3
	2/3 Avrami Erofeev	[-ln(1-α)]$^{2/3}$	A4

© 2026 by the author(s). Distributed under a Creative Commons CC BY license.

Preprints.org (www.preprints.org) | NOT PEER-REVIEWED | Posted: 3 March 2026 doi:10.20944/preprints202603.0200.v1

Thermodynamic parameters including enthalpy change (ΔH), Gibbs free energy change (ΔG), and entropy change (ΔS) were derived from activation energy values and pre-exponential factors obtained through the Coats-Redfern kinetic model. The maximum decomposition temperature for each blend was used in the thermodynamic computations. The following equations were applied:

$$\Delta H = Ea - RT \quad (4)$$

$$\Delta G = Ea + RT_m^{\ln\left(\frac{K_b T}{hA}\right)} \quad (5)$$

$$\Delta S = \frac{\Delta H - \Delta G}{T_m} \quad (6)$$

where R is the gas constant (0.008314 kJ / mol K), K_b is Boltzmann's constant (1.381×10^{-23} m^2 kg/s^{-2} K^{-1}), h is Planck's constant ($6.626 \times 10{-}34$ m^2 kg/s), and T_m is the maximum temperature at which decomposition occurs. These dictate the energy requirements and spontaneity of the pyrolysis reactions under catalytic conditions.

3. Results and Discussion

Table 2 shows the summary of the results from the HTC experiments.

3.1. Co-HTC Results of CS-LDPE Samples and Statistical Analysis

Table 2. Summary of Experimental Runs and Results.

Temperature, °C	Residence Time, min	Mass Yield, %
240	30	45.7180
220	45	49.0931
200	60	53.2232
248.3	45	37.4909
220	45	48.5461
220	45	48.6707
240	60	38.8179
220	45	46.6872
220	66.2	46.1064
220	23.8	46.2120
191.7	45	49.7985
220	45	46.9162
200	30	45.0310

Table 3. ANOVA for HTC conditions at 95% confidence level.

Source	Sum of squares	df	Mean Square	F-value	p-value
Model	206.67	5	41.33	35.88	<0.0001
A-Temperature	121.09	1	121.09	105.10	<0.0001
B-Residence Time	0.16322	1	0.1632	0.1417	0.7178
AB	56.94	1	56.94	49.43	0.0002
A^2	27.00	1	27.00	23.44	0.0019
B^2	3.53	1	3.53	3.07	0.1233
Residual	8.06	7	1.15		
Lack-of-fit	3.23	3	1.08	0.8885	0.5195
Pure Error	4.84	4	1.21		
Cor Total	214.73	12			

The two-way ANOVA suggested a quadratic model with an R^2 value of 0.9624 which means that 96.24% of the variability in the % mass yield data can be explained by the quadratic model, indicating

© 2026 by the author(s). Distributed under a Creative Commons CC BY license.

Preprints.org (www.preprints.org) | NOT PEER-REVIEWED | Posted: 3 March 2026 doi:10.20944/preprints202603.0200.v1

a good fit for predicting % mass yield values given reaction parameters. With an F-value of 35.88, there is only <0.01% chance that this could occur due to noise. This indicates that the model used is significant. Fit statistics of this model further reveals a predicted R^2 of 0.8580 which is in reasonable agreement with the adjusted R^2 of 0.9356, giving a difference of less than 0.2. Furthermore, the adequate precision is 21.019. This measures the signal to noise ratio of which desirable figure should be greater than 4. The lack-of-fit F-value is 0.89 with a 51.95% chance that this could occur due to noise. Non-significant lack-of-fit is good as this ascertains fitting of the model. All of these support the credibility of the model to navigate the design space.

P-values less than 0.0500 indicate model terms are significant. In this case, temperature and the interaction of both factors are significant model terms. As for temperature (A), it is well documented that it is the most significant parameter affecting hydrochar yield. It has a negative effect to mass yield such that increasing it reduces solid return of hydrochar, as shown in Figure 1.

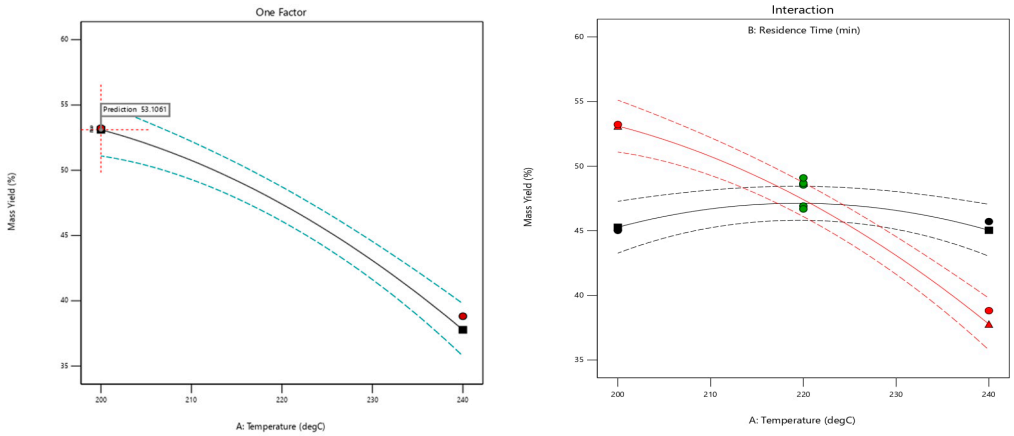

Figure 1. Stacked normalized IR spectra of undersized hydrochar, oversized hydrochar, oversized LDPE.

The interactive effect of temperature and residence time (AB) was also found to be significant on hydrochar yield. At shorter residence time, hydrochar yield does not significantly change as temperature is increased as indicated by the LSD bars. However, at longer periods, increasing the temperature decreases hydrochar mass yield.

3.2. Optimization and Validation of Co-HTC Process Conditions

Upon optimization of the reaction parameters to maximize the % mass yield, the optimum reaction temperature and residence time was determined to be 200 °C and 60 minutes, respectively, with a desirability of 0.993. By statistical analysis and significance, these optimized parameters predict a mass yield of 53.106%. Additional two separate co-HTC runs were performed following these optimized parameters. These gave mass yields of 52.2146% and 51.1415%, revealing a -2.69% average deviation. This relatively small deviation affirms that the model effectively captures the system behavior and can be used to reliably predict outcomes in hydrothermal carbonization of CS and LDPE.

3.3. Characterization of Optimum Hydrochar Fractions

3.3.1. Fuel Analysis of Optimum Hydrochar

HTC significantly increased the FC of cacao shell to hydrochar, as well as decreased its volatile matter, ash, and moisture contents. The optimum hydrochar also possesses lower H and O contents and higher C from its biomass parent which in turn elevated its measured HHV of 21.22 MJ/kg, making the carbonization effective and improving its fuel characteristics. The high C content of LDPE may have been contributor to the added carbon concentration of optimum hydrochar.

© 2026 by the author(s). Distributed under a Creative Commons CC BY license.

Preprints.org (www.preprints.org) | NOT PEER-REVIEWED | Posted: 3 March 2026 doi:10.20944/preprints202603.0200.v1

Table 3. Ultimate and Proximate composition of Optimum Hydrochar.

Element	Ultimate Analysis					Proximate Analysis				HHV (MJ/kg)
	C (%)	H (%)	O (%)	N (%)	S (%)	M (%)	FC (%)	VM (%)	Ash (%)	
Cacao Shell*	39.87	5.96	45.33	0.74	0.13	12.66	18.42	60.95	7.97	16.20
Optimum Hydrochar	56.17**	5.02**	31.84**	6.97**	-	2.52	31.40	60.04	6.04	21.11
LDPE***	93.76	5.74	0.50	-	-	1.20	-	98.30	0.50	40.60

* Adeboye, et. al. (2022); ** Nuchhen estimation; *** Adejanyu (2022).

3.3.2. Functional Group Analysis of Hydrochar Fractions

In Figure 2, stacked FTIR spectra provide compelling evidence of Undersized Hydrochar, Oversized Hydrochar, and Oversized LDPE samples resulting from the co-HTC treatment. The analysis of these spectra reveals fascinating insights into the materials post-treatment. The Undersized Hydrochar, for instance, presents a classic fingerprint of biomass-derived hydrochar, indicating that the de-oxygenation and aromatization processes, have successfully occurred, yet it crucially retains significant amounts of oxygen-containing functional groups (as evidenced by prominent O-H and C-O stretches in the spectral data) [15,16]. Similarly, the Oversized Hydrochar exhibits a highly consistent chemical nature to its undersized counterpart. While subtle differences in relative peak intensities might hint at slight variations in the degree of carbonization, specific functional group content, or the concentration of inorganic matter, possibly tied to different particle sizes or densities achieved during separation, their overall chemical identity as hydrochar remains highly consistent [17].

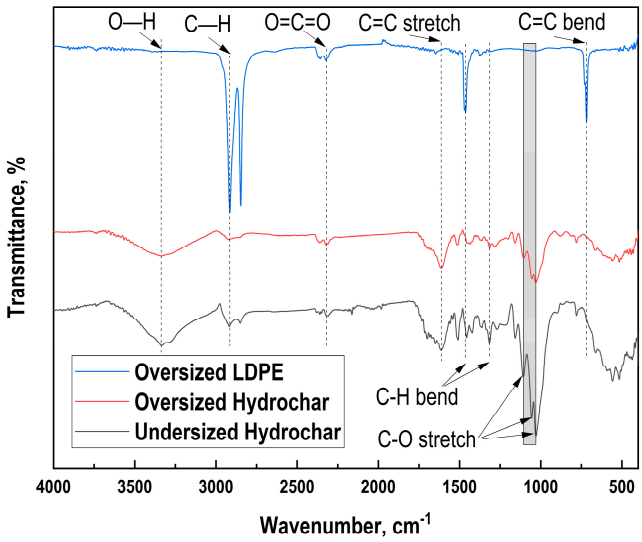

Figure 2. Stacked normalized IR spectra of undersized hydrochar, oversized hydrochar, oversized LDPE.

The hydrochar fractions are rich in oxygen-containing groups and aromatic structures, evidently found in fingerprint regions, which is consistent with the transformation of biomass during HTC [18]. The LDPE fraction is almost exclusively aliphatic hydrocarbons, confirming its nature as polyethylene. This suggests that polyethylene did not completely degrade. Meanwhile, both the Undersized and Oversized Hydrochar fractions show very similar functional group profiles, although distinct peaks are evident in the Oversized hydrochars which is potentially influenced by the particle sizes and residues from co-HTC treatment with LDPE.

© 2026 by the author(s). Distributed under a Creative Commons CC BY license.

Preprints.org (www.preprints.org) | NOT PEER-REVIEWED | Posted: 3 March 2026 doi:10.20944/preprints202603.0200.v1

3.3.3. Surface Morphology

The Undersized Hydrochar shows an irregular, rough, and highly porous surface structure of undisturbed fiber. This is indicative of the decomposition and re-polymerization reactions after HTC treatment, which forms a carbonaceous network with varying degrees of porosity and surface roughness [19]. The porous structure suggests high surface area, which is advantageous for energy applications. The absence of melting or fused structures further confirms minimal influence from LDPE in this fraction. The Oversized Hydrochar presented a heterogeneous and more irregular and coarse structure under SEM imaging. Compared to the undersized sample, this fraction showed a mix of porous and dense regions. These features suggest partial melting or fusion, potentially indicating the interaction between the biomass and LDPE during co-hydrothermal carbonization. The irregularity in the structure hints at uneven heat transfer or incomplete decomposition, which is common when plastics are blended with wet biomass in thermal processes.

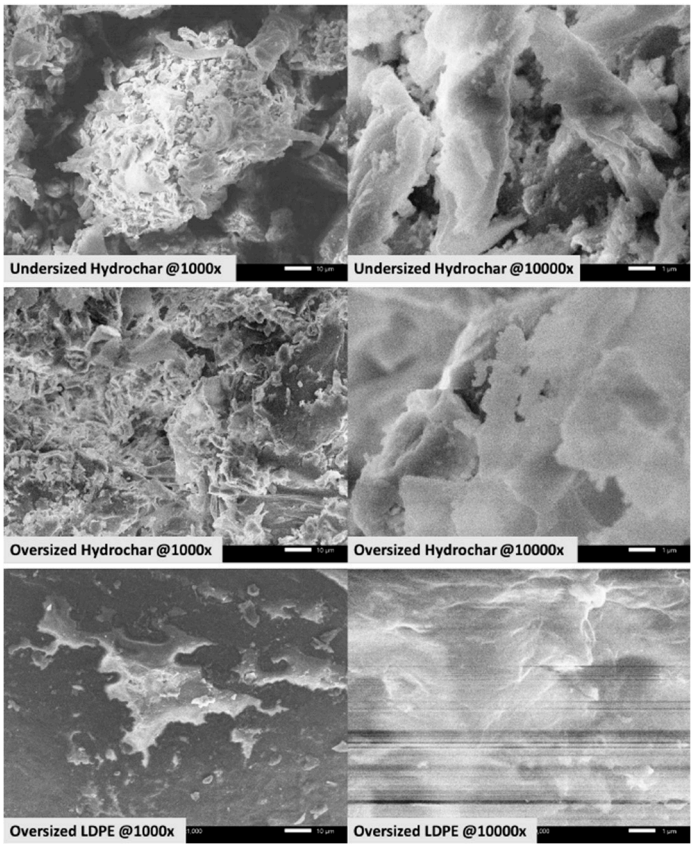

Figure 3. Micrograph (SEM images) obtained for Hydrochar fractions after Co-HTC treatment.

In contrast, the SEM images of the Oversized LDPE sample presented a smooth, homogeneous, and slightly glossy surface, lacking the fibrous and porous characteristics seen in Undersized and Oversized samples. The uniformity in the texture suggests melting and resolidification of LDPE during co-hydrothermal carbonization at 200 °C, which is below its full decomposition temperature but enough to soften or fuse the plastic, which corroborated with the FTIR findings. No structural indications of biomass integration were visible, pointing to physical phase separation between plastic and organic matter during the co-hydrothermal carbonization process. This suggests that co-HTC can be used as a separation method for mixed waste involving plastics and biomass.

3.3.4. Elemental Analysis

Table 4 presents the elemental composition of Undersized Hydrochar, Oversized Hydrochar, and Oversized LDPE, revealing distinct differences reflecting feedstock interactions during co-HTC

© 2026 by the author(s). Distributed under a Creative Commons CC BY license.

Preprints.org (www.preprints.org) | NOT PEER-REVIEWED | Posted: 3 March 2026 doi:10.20944/preprints202603.0200.v1

treatment. Carbon content notably increases with particle size within 83.79% to 99.19%, with Oversized LDPE exhibiting the highest carbon purity, consistent with its characteristic polymer [20]. Oversized hydrochar also shows higher carbon content than Undersized hydrochar, indicating the influence of incorporated polymer residues and potentially the presence of inorganic elements [21].

Furthermore, a couple of trace elements (S, K, Ca, Zn) were detected inherent from the feedstocks. Undersized hydrochar contains K, Ca, and Zn, which tend to accumulate in the solid residue during co-HTC due to their low volatility. K and Ca are common ash-forming elements in plant biomass, while Zn is a known trace micronutrient [20]. Interestingly, only Ca was detected in Oversized hydrochar, likely from CS ash agglomerates [21]. In Oversized LDPE, only traces of S and K were found. The lowered concentration of K, compared to Undersized hydrochar, confirms biomass interaction during co-HTC, while the small amount of S suggests an additive in the commercial LDPE that remained unconverted, potentially influenced by hydrocarbon-based treatment [21].

Table 4. EDX mean elemental composition of Hydrochar Fractions.

Element	C (%)	S (%)	K (%)	Ca (%)	Zn (%)
Undersized Hydrochar	83.79	-	9.08	2.74	4.39
Oversized Hydrochar	90.4	-	-	9.6	-
Oversized LDPE	99.19	0.8	1.28	-	-

3.4. Thermal Degradation Analysis of Optimized Hydrochar

3.4.1. Thermal Decomposition Behavior

The thermal decomposition characteristics of the Undersized Hydrochar, Oversized Hydrochar and the Oversized LDPE were analyzed via pyrolysis in TGA with corresponding sample parameters: test type - thermal stability test, temperature of 40 to 650 °C, N_2 gas flow rate of 20 mL/min, heat flow rate of 20 °C/min. The analysis illustrated differences in degradation temperature for both hydrochars and the oversized LDPE. The TGA and DTG curves, mass (%) loss with respect to temperature, of hydrochar fractions overlap and are shown for comparison. Figure 4 illustrates the TGA/DTG curves of these hydrochar fractions.

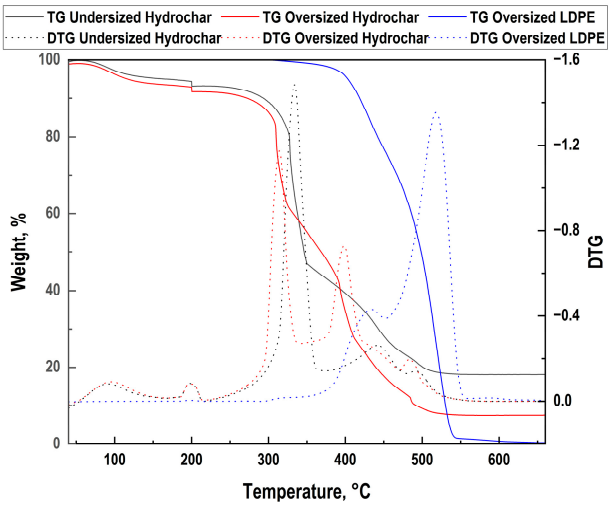

Figure 4. TG/DTG Curves of undersized hydrochar, oversized hydrochar and oversized LDPE.

In the low-temperature region (50–100 °C), minimal weight loss was observed, corresponding to the evaporation of residual moisture and free water, primarily from the hydrochar fractions. Between 100–150 °C, a slight mass reduction was detected in the hydrochars, potentially due to the release of low-molecular-weight volatile organics derived during HTC, while LDPE remained

© 2026 by the author(s). Distributed under a Creative Commons CC BY license.

Preprints.org (www.preprints.org) | NOT PEER-REVIEWED | Posted: 3 March 2026 doi:10.20944/preprints202603.0200.v1

thermally stable due to its hydrophobic and chemically inert structure. The enhanced thermal reactivity of undersized hydrochar (steeper slope) is likely due to its larger surface area and more exposed functional groups compared to Oversized hydrochar [22].

The most significant mass loss occurred in the 250–350 °C range, where both hydrochar fractions began active pyrolysis, as evidenced by a sharp weight reduction. This region corresponds to the thermal decomposition of remaining cellulose and hemicellulose-derived intermediates in the hydrochar, while LDPE began to soften and undergo initial chain scission. Complete degradation of LDPE occurred in the 350–550 °C range, marked by a steep mass drop at ~424 °C, remarks early degradation process than its typical decomposition behavior (about 457 °C) [23]. Meanwhile, the hydrochar fractions continued to decompose, primarily through lignin breakdown and secondary cracking reactions.

These results confirm that co-HTC pre-treatment significantly stabilizes the feedstock and enables staged decomposition during pyrolysis. LDPE enhances the carbon richness and thermal reactivity of the hydrochar, while cacao shell biomass contributes structure and porosity. The combined effect promotes cleaner, energy-dense hydrochar and potentially higher bio-oil or syngas yields during pyrolysis. This synergistic behavior aligns with previous findings by Khan et al. (2020) and Liu et al. (2022), who emphasized the role of plastic-biomass blends in improving thermochemical conversion outcomes [24,25].

The DTG analysis provides valuable insight into the thermal decomposition behavior of the hydrochar fractions and LDPE after co-HTC. The undersized hydrochar exhibited two major degradation peaks: one at approximately 310 °C, corresponding to the decomposition of volatile organics and hemicellulose-cellulose-derived intermediates, and a second, broader peak around 410 °C, associated with the breakdown of thermally stable lignin structures. The higher peak intensity and earlier onset for Undersized hydrochar suggest faster overall degradation kinetics, potentially due to its larger surface area and reactivity. The oversized hydrochar followed a similar two-stage pattern, one though the peaks (~310 °C) was slightly sharper and shifted, while the second peak at approximately 390 °C which tend to overlap the undersized hydrochar, indicating a more homogeneous carbon matrix likely influenced by increased LDPE content. The Oversized hydrochar's peak occurring slightly later and being less intense reflects slower heat diffusion and possibly more thermally stable intermediates, influenced by its larger particle size and potentially different structural modifications during co-HTC [26].

In contrast, the LDPE sample demonstrated a single, intense degradation peak around 490 °C, which aligns with the characteristic pyrolytic breakdown of polyolefin chains. This rapid decomposition is typical of LDPE's thermal cracking, yielding alkenes and paraffinic compounds with minimal char residue as investigated by the study of Das and Tiwari (2017) [27]. The sharper degradation transitions observed in LDPE-containing hydrochar suggest that the inclusion of plastic during HTC affects not only the thermal stability of the resultant hydrochar but also its devolatilization kinetics during pyrolysis. Furthermore, the enhanced carbonization and energy density observed in DTG peaks support the viability of co-HTC as a pretreatment for thermochemical valorization of mixed organic-plastic waste streams.

3.4.2. Kinetic and Thermal Parameters

The Coats–Redfern method was used to calculate pyrolysis kinetic and thermal parameters (Equation (2)). The kinetic parameters were derived using the Coats–Redfern method, assuming a simplified single-step reaction mechanism. Table 5 shows the kinetic parameters obtained for the individual pyrolysis of Undersized Hydrochar, Oversized Hydrochar, and Oversized LDPE samples during the devolatilization stage at 240-519 °C. The model with the highest R^2 was selected as estimated activation energy for each type of hydrochar fraction.

© 2026 by the author(s). Distributed under a Creative Commons CC BY license.

Preprints.org (www.preprints.org) | NOT PEER-REVIEWED | Posted: 3 March 2026 doi:10.20944/preprints202603.0200.v1

Table 5. Activation Energy (Ea) and Reaction Model for Pyrolysis of the Hydrochar Fractions.

Sample	Ea (kJ/mol)	Reaction Model	R^2 (%)
Undersized Hydrochar	43.085	R1	92.347
Oversized Hydrochar	38.484	R1	96.931
Oversized LDPE	120.896	R1	98.196

The TG and DTG of the hydrochar fractions were analyzed by the CR method. All 16 solid-state reaction models have been fitted into Equation (2). The model with the highest correlation (largest R^2 value) indicates the best-fitted linear line, which will be selected as the most appropriate model to describe the reaction. From the results, the first-order model consistently achieved the highest R^2 for all hydrochar fractions among all other models. Utilizing the model, the Ea was calculated at 43.084 kJ/mol for undersized hydrochar, 38.484 kJ/mol for oversized hydrochar, and 120.896 kJ/mol for oversized LDPE.

The lower apparent activation energy of undersized hydrochar compared with the oversized hydrochar implies that particle size dictates the thermal stability of hydrochar. Lower particle-sized hydrochar exhibited higher resistance to bond breaking once initiated. Smaller particles have increased surface area and reactive site density, but this heightens intraparticle diffusion resistance for evolved volatiles during pyrolysis, raising the effective Ea due to particle-size-dependent heat transfer efficiency [28]. Larger particles allow easier volatile escape, lowering diffusion barriers and thus Ea for intrinsic decomposition [29].

The subsequent lower activation energy of undersized and oversized hydrochars indicate that these fractions involve easily decomposable volatiles, potentially a characteristic of porous solid-state reactions [35]. In contrast, Oversized LDPE possesses a much higher activation energy, characteristic of the stable materials that requires robust thermal degradation of its long-chain polyethylene requiring significant energy to break the strong C-C bonds through random chain scission or depolymerization [30].

Table 6. Thermokinetic parameters for Pyrolysis of the Hydrochar Fractions.

Sample	T_{max}	E_a $(\frac{kJ}{mol})$	ΔH $(\frac{kJ}{mol})$	ΔG $(\frac{J}{mol})$	ΔS $(\frac{J}{mol\ K})$	A (min^{-1})
Undersized	334.61	43.085	38.033	1.826E+05	-237.931	769.311
Oversized	314.50	38.484	33.600	1.774E+05	-244.830	324.758
Oversized LDPE	518.06	120.896	114.319	2.284E+05	-144.218	7.87E+07

Reinforcing the earlier observation on the undersized and oversized hydrochars, the lowering of activation energy alongside increase of particle size is supported by decreased frequency collision. The surface area loss reduced collision frequency often from steric hindrance. This slows the overall rate despite potentially lower Ea, common in treated mixed materials where cross-linking restricts chain mobility [31]. However, despite lower A, oversized hydrochar displayed lower Tmax than that of undersized hydrochar which is uncommon as decreased A typically shifts the Tmax to higher values in pyrolysis kinetics. This trend deviation may be attributed to the treated LDPE residues mixing to the hydrochars. Metal impurities from LDPE lower the energy barrier more than A restricts frequency by providing alternative low-energy reaction pathways. Presence of Ca in oversized hydrochar as shown in Table 4 may have acted as a base catalyst and stabilizes intermediates, often dominating over low A to lower Tmax. Undersized hydrochar may have possessed alkalis K and Ca but its Zn content cancels catalytic effect.

Oversized LDPE exhibited a high Ea of 120.896 kJ/mol, a characteristic value associated with the cleavage of C–C bonds in long-chain polyethylene structures [32]. This process aligns with random chain scission mechanisms, commonly reported in polyolefin pyrolysis. The high A in oversized LDPE indicates rapid degradation once the activation threshold is reached.

© 2026 by the author(s). Distributed under a Creative Commons CC BY license.

Preprints.org (www.preprints.org) | NOT PEER-REVIEWED | Posted: 3 March 2026 doi:10.20944/preprints202603.0200.v1

The remaing thermodynamic values across samples support the non-spontaneous and endothermic nature of pyrolysis, requiring external energy to sustain decomposition.

From Table 7, it can be observed that the thermal degradation peak temperature virtually remains unchanged but with a large difference on the apparent activation energy. From an activation energy of raw LDPE at 242.9 kJ/mol, the hydrothermally-treated LDPE has relatively lower thermal stability at an activation energy of 128.85 kJ/mol. This reinforces the effectivity of the hydrothermal treatment to destabilize LDPE and make it more easily susceptible to inner bond breakage when subjected to thermal regime [33].

Table 7. Comparative analysis of Oversized LDPE with raw LDPE in TGA.

Samples	T_{max} (°C)	Ea (kJ/mol)
Oversized LDPE	518.06	128.85
Raw LDPE (Adeboye et al., 2022)	519	242.9

4. Conclusions

The study conducted showed the feasibility and advantages of utilizing hydrochar derived from the co-HTC of cacao shell and low-density polyethylene (LDPE) as a waste management mechanism of biomass-plastic waste blends for pyrolytic application. Morphological analysis through SEM-EDX revealed distinct surface features across the three hydrochar fractions supporting the effectiveness of sieving as a separation method. The elemental analysis confirmed the presence of both organic (biomass) and inorganic (polymer) elements, aligning with the expected carbon content increases with particle size within 83.79% to 99.19% of fractions. FTIR analysis confirmed the presence of both biomass (cellulose/lignin) and plastic-derived (polyethylene structures) functional groups in the hydrochar fractions indicating chemical interaction and partial degradation of LDPE during co-HTC. And lastly, TGA showed that the produced hydrochar exhibited enhanced thermal stability and altered pyrolysis kinetics compared to untreated biomass. Moreover, the activation energy values and thermal decomposition profiles indicate favorable characteristics for bio-oil production and energy recovery. Furthermore, studies that utilize hydrothermal carbonization as a thermal degradation process can also be done for other types of plastics and biomass. Future research is also needed to improve its efficiency for real-world application.

Author Contributions: Writing – original draft, M.F.A.; Writing – review and editing, M.F.A.; Visualization, Software, Data Validation, A.P.D.P.; Data Curation, Q.M.I., C.O., A.B., R.M.M., and J.S.; Methodology, K.M.U. and J.M.T.; Validation, R.G. and R.R.A.; Conceptualization, A.M.; Funding acquisition, A.M. All authors have read and agreed to the published version of the manuscript.

Funding: This research was funded by the Department of Science and Technology - Philippine Council for Industry, Energy, and Emerging Technology Research and Development (DOST-PCIEERD).

Data Availability Statement: The authors confirm that all data used in this study are openly available within the article. Further inquiries can be directed to the corresponding authors.

Acknowledgments: The authors would like to acknowledge the immense support of the Department of Science and Technology - Philippine Council for Industry, Energy, and Emerging Technology Research and Development (DOST-PCIEERD) for the research funding, and to the Mindanao State University – Iligan Institute of Technology for providing the laboratory facilities, equipment, analyses, and materials for the researchers.

Conflicts of Interest: The remaining authors declare that the research was conducted in the absence of any commercial or financial relationships that could be construed as a potential conflict of interest.

© 2026 by the author(s). Distributed under a Creative Commons CC BY license.

Preprints.org (www.preprints.org) | NOT PEER-REVIEWED | Posted: 3 March 2026 doi:10.20944/preprints202603.0200.v1

References

1. Rafey, A., & Siddiqui, F. Z. (2023). A review of plastic waste management in India – challenges and opportunities. International Journal of Environmental Analytical Chemistry, 103(16), 3971–3987. https://doi.org/10.1080/03067319.2021.1917560
2. Chamas A., Moon, H., Zheng, J., Qiu, Y., Tabassum, T., Jang, JH., Abu-Omar, M., Scott, S., Suh, S. Degradation rates of plastics in the environment. ACS Sustainable Chemistry & Engineering. https://doi.org/10.1021/acssuschemeng.9b06635
3. Dingding Yao, He Li, Babu Cadiam Mohan, Arun Kumar Prabhakar, Yanjun Dai, and Chi-Hwa Wang. ACS Sustainable Chemistry & Engineering 2022 10 (3), 1125-1136. https://doi.org/10.1021/acssuschemeng.1c05945
4. Jambeck JR, Geyer R, Wilcox C, Siegler TR, Perryman M, Andrady A, Narayan R, Law KL. Marine pollution. Plastic waste inputs from land into the ocean. Science. 2015 Feb 13;347(6223):768-71. doi: 10.1126/science.1260352. PMID: 25678662.
5. Ghatge, S., Yang, Y., Ahn, JH. et al. Biodegradation of polyethylene: a brief review. Appl Biol Chem 63, 27 (2020). https://doi.org/10.1186/s13765-020-00511-3
6. Suganthi, R., Saravanan, R., Brundha, A., Bowya, T., Lakshmi, A. J., Abirami, P., & Ashwini, M. (2024). Novel approaches in processing of cacao byproducts and their applications for a sustainable future. 235–255. https://doi.org/10.4324/9781003381761-15
7. Arellano, O., Flores, M., Guerra, J., Hidalgo, A., Rojas, D., & Strubinger, A. (2016b). Hydrothermal carbonization of corncob and characterization of the obtained hydrochar. DOAJ (DOAJ: Directory of Open Access Journals). https://doi.org/10.3303/cet1650040
8. YaFei S. (2020). A review on hydrothermal carbonization of biomass and plastic wastes to energy products. Biomass and Bioenergy (134). Elsevier. doi: 10.1016/j.biombioe.2020.105479
9. Islam, M. T., Reza, T., Klinger, J., & Saha, N. (2021). Co-Hydrothermal Carbonization (Co-HTC) of Biomass-Plastic Blend: Enhancement of Fuel Quality. AIChE Annual Meeting Proceedings.
10. Wang, R., Wang, Y., Zhang, Y., & Chen, H. (2023). Influence of Hydrothermal Carbonization on Catalytic Fast Pyrolysis of Agricultural Biomass. Applied Sciences, 13(7), 4190. https://doi.org/10.3390/app13074190
11. Ye, L., Zhang, J., Wang, G., Wang, C., Mao, X., Ning, X., Zhang, N., Teng, H., Li, J., & Wang, C. (2023). Feasibility analysis of plastic and biomass hydrochar for blast furnace injection. Energy, 263, 125903. https://doi.org/10.1016/j.energy.2022.125903
12. Adeboye, B., Idris, M., Adedeji, W., Kayode, O., Adefajo, A., & Rabiu, K. (2022). Thermogravimetric Analysis and Kinetic Study on the Pyrolysis of Some Post-Consumer Plastic Wastes. Premier Journal of Engineering and Applied Sciences, 1-9.
13. Nhuchhen, Daya. (2016). Prediction of carbon, hydrogen, and oxygen compo-sitions of raw and torrefied biomass using proximate analysis. Fuel. 180. 348-356. 10.1016/j.fuel.2016.04.058.
14. Adeyanju, Anthony. (2022). Comparisons of Cocoa Pod Husks and other Biomass Wastes for Syngas Production. E3S Web of Conferences. 336. 00037. 10.1051/e3sconf/202233600037.
15. Magdziarz, A., Wolf, M., & Wądrzyk, M. (2020). Pyrolysis of hydrochar derived from biomass – Experimental investigation. Fuel, 267, 117246. https://doi.org/10.1016/j.fuel.2020.117246
16. Wu, S., Wang, Q., Cui, D., Sun, H., Yin, H., Xu, F., & Wang, Z. (2023). Evaluation of fuel properties and combustion behaviour of hydrochar derived from hydrothermal carbonisation of agricultural wastes. Journal of the Energy Institute. https://doi.org/10.1016/j.joei.2023.101209
17. Teribele, T., Costa, M. E. G., Pereira, L. M., Bernar, L. P., de Castro, D. A. R., Assunção, F. P. d. C., Santos, M. C., Brandão, I. W. d. S., Schultze, M., Hofmann, T., & Machado, N. T. (2023). Hydrothermal carbonization of corn stover: Structural evolution of hydrochar and degradation kinetics. Energies, 16(7), 3217. https://doi.org/10.3390/en16073217
18. Waseem, R., Gupta, A. K., & Kumar, P. (2023). Agricultural Waste Management by Hydrothermal Carbonization. IARS International Research Journal, 12(2), 215.
19. Canopoli, L., Coulon, F., Wagland, ST. (2019). Degradation of excavated polyethylene and polypropylene waste from landfill. Science of the Total Environment. Elsevier. https://doi.org/10.1016/j.scitotenv.2019.134125

© 2026 by the author(s). Distributed under a Creative Commons CC BY license.

Preprints.org (www.preprints.org) | NOT PEER-REVIEWED | Posted: 3 March 2026 doi:10.20944/preprints202603.0200.v1

20. Ainali, N., Bikiaris, D., Lambropoulou, D. (2021). Aging effects on low- and high-density polyethylene, polypropylene and polystyrene under UV irradiation: An insight into decomposition mechanism by Py-GC/MS for microplastic analysis. Journal of Analytical and Applied Pyrolysis 158: 105207. https://doi.org/10.1016/j.jaap.2021.105207
21. Khan, R. M., Mushtaq, A., Israr, A., & Nafees, A. (2019). Comparative study for melt flow index of high density polyethylene, low density polyethylene and linear low density polyethylene. Pakistan Journal of Engineering and Applied Sciences.
22. Li, L., Liu, Y., Lv, Y., Zhang, S., & Li, C. (2018). Hydrothermal carbonization of municipal solid waste: Effects of operating parameters on hydrochar properties and energy recovery. Energy Conversion and Management, 171, 1485-1492.
23. Upare, D. P., Lee, C. W., Lee, D. K., & Kang, Y. S. (2024). Effect of acidity of solid acid catalysts during non-oxidative thermal decomposition of LDPE. Carbon Letters, https://doi.org/10.1007/s42823-024-00789-z
24. Khan, M. M., Shamim, T., & Hussain, A. (2020). Conversion of agricultural residues into biochar and hydrochar: A review on co-hydrothermal carbonization. Energy Conversion and Management, 205, 112340. https://doi.org/10.1016/j.enconman.2019.112340
25. Liu, H., Zhang, L., Zhang, J., Liu, Z., & Ma, D. (2022). Combustion behavior and kinetics of hydrochars derived from different biomass feedstocks. Journal of Analytical and Applied Pyrolysis, 163, 105465. https://doi.org/10.1016/j.jaap.2022.105465
26. Li, L., Liu, Y., Lv, Y., Zhang, S., & Li, C. (2018). Hydrothermal carbonization of municipal solid waste: Effects of operating parameters on hydrochar properties and energy recovery. Energy Conversion and Management, 171, 1485-1492.
27. Das, P., & Tiwari, P. (2017). Thermal degradation kinetics of plastics and model selection. Thermochimica Acta, 654, 191–202. https://doi.org/10.1016/j.tca.2017.06.001
28. Li, L., Liu, Y., Lv, Y., Zhang, S., & Li, C. (2018). Hydrothermal carbonization of municipal solid waste: Effects of operating parameters on hydrochar properties and energy recovery. Energy Conversion and Management, 171, 1485-1492.
29. Pum, D., Stelzer, N., & Dietrich, K. (2020). Reaction and diffusion kinetics during hydrothermal carbonization by means of SEM–EDX analysis. Industrial & Engineering Chemistry Research, 59(17), 6642–6652. https://doi.org/10.1021/acs.iecr.9b05643
30. Wang, Z., Wang, X., Lin, Y., Yang, J., Chen, R., & Liu, D. (2018). Thermal degradation characteristics and kinetics of typical lignocellulosic biomass components using TGA-FTIR. Bioresource Technology, 269, 201-209.
31. Gulab, H., Khan, M. J., Butt, M. S., Ahmad, T., & Khan, M. I. (2021). Thermal degradation kinetics of low-density polyethylene (LDPE) and polypropylene (PP) waste using thermogravimetric analysis (TGA). Waste Management, 120, 683-690.
32. Patil Y, Ku X, Vasudev V. Pyrolysis Characteristics and Determination of Kinetic and Thermodynamic Parameters of Raw and Torrefied Chinese Fir. ACS Omega. 2023 Sep 15;8(38):34938-34947. doi: 10.1021/acsomega.3c04328. PMID: 37779928; PMCID: PMC10536841.
33. Espina, S., Alvarez, R., Diez, M. and Casal, M. (2015). Coal and Plastic Waste Co-pyrolysis by Thermal Analysis–mass Spectrometry. Fuel Processing Technology, 137: 351-358.

Disclaimer/Publisher's Note: The statements, opinions and data contained in all publications are solely those of the individual author(s) and contributor(s) and not of MDPI and/or the editor(s). MDPI and/or the editor(s) disclaim responsibility for any injury to people or property resulting from any ideas, methods, instructions or products referred to in the content.

© 2026 by the author(s). Distributed under a Creative Commons CC BY license.